Available *online* at: https://journal.gioarchitect.co.id/index.php/localengineering/issue/current

Local Engineering

Journal of Local Architecture and Civil Engineering

| Doi: 10.59810/localengineering | ISSN (Online) 2987-7555 |

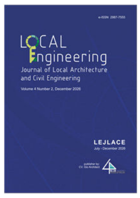

Civil Engineering – Research Article

Evaluation of Infiltration, Surface Runoff, and Land Cover Change Sensitivity Based on The Horton Model in an Urban Campus Area: A Case Study of Unwira Kupang

Agustinus Haryanto Pattiraja[1], *Irene Veronika sare Muda*[1], *Mauritius Ildo Rivendi Naikofi*[1], *Peregrius Dhae Siga Taa*[1, 2]

[1]*Department of Civil Engineering, Faculty of Engineering, Universitas Katolik Widya Mandira, Indonesia*

[2]*Civil Engineering, School of Engineering and Science, Dili Institute of Technology, Dili, Timor Leste*

ARTICLE INFORMATION

Received: June 18, 2026

Revised: August 02, 2026

Available online: September 19, 2026

KEYWORDS

Horton model, infiltration, land cover change

CORRESPONDENCE

Agustinus Haryanto Pattiraja

E-mail: agustinuspattiraja@unwira.ac.id

A B S T R A C T

Changes in land cover within urban areas can reduce infiltration capacity and increase surface runoff. This study aims to evaluate infiltration rates, surface runoff, and the sensitivity of land cover changes within the core area of the Widya Mandira Catholic University (UNWIRA) Kupang campus using the Horton Model. Field measurements were conducted using a double-ring infiltrometer at three observation points representing vegetated land, semi-permeable surfaces, and impervious/built-up areas. The Horton parameters were calibrated through nonlinear optimization by minimizing the Root Mean Square Error (RMSE), after which they were applied to estimate cumulative infiltration over a 60-minute period. Surface runoff was estimated based on design rainfall with return periods of 2, 5, and 10 years, while sensitivity analysis was performed through scenarios involving a 1–5% reduction in permeable land area. The calibration results produced RMSE values ranging from 0.894 to 2.001 cm/hour. Zone 2 exhibited the greatest infiltration capacity, reaching 2,405.42 m³, whereas Zone 3 had the lowest infiltration capacity, 618.33 m³, and generated the highest R_{10} runoff volume of 1,090.07 m³. Under the scenario involving a 5% reduction in permeable area, runoff in Zone 1, Zone 2, and Zone 3 increased by 8.28%, 18.87%, and 2.84%, respectively. These findings indicate that Zone 2 is the most sensitive in relative terms, whereas Zone 3 is the most vulnerable based on its actual runoff volume. Overall, the results underscore the importance of preserving permeable areas and enhancing infiltration facilities in future campus development.

INTRODUCTION

Infiltration is one of the fundamental processes within the hydrological cycle that plays a critical role in maintaining water resource balance, particularly in the context of stormwater management in urban environments. The infiltration rate reflects the soil's capacity to absorb rainfall into its pore spaces and directly influences the volume of rainfall that is converted into surface runoff. When soil is unable to absorb rainfall efficiently, excess rainfall becomes surface runoff, potentially resulting in ponding or localized flooding.

The Horton Model is among the most widely used empirical infiltration models because of its simplicity and its ability to describe the exponential decline in infiltration rate over time (Horton 1941). The model assumes that the infiltration rate decreases from its initial value (f_0) toward a constant infiltration rate (f_c) as time progresses due to increasing soil saturation (Yang, Zhang, and Pan 2020). Numerous studies have demonstrated the effectiveness of this model in representing infiltration under a wide range of land-use conditions.

Bagus et al. (2022), Annisa (2018), and Suryanto (2017) demonstrated that the Horton Model can accurately represent infiltration rates across various land-use types while remaining relatively straightforward to implement and calibrate. Within urban environments, Felix and Sentosa (2020) and Christian and Pranoto (2021) emphasized that limited soil infiltration capacity, combined with inadequate drainage system capacity, can significantly increase surface runoff and the risk of urban flooding. Consequently, infiltration assessment should be integrated into flood mitigation and urban drainage planning.

Based on this background, the present study was conducted to evaluate infiltration capacity, surface runoff generation, and the sensitivity of land cover change using the Horton Model within the core area of the UNWIRA Kupang campus.

RESEARCH METHODS

This study was conducted at the Widya Mandira Catholic University (UNWIRA) Kupang campus, located in Penfui Timur Village, Kupang Tengah District, Kupang Regency. Although the campus is administratively situated within the regency, it forms part of the urban agglomeration of Kupang City, characterized by a mixed land-use pattern consisting of built-up areas and open spaces. Field infiltration tests were carried out using a double-ring infiltrometer at three observation points representing vegetated land, semi-permeable areas, and built-up surfaces. Although the university occupies an administrative area of approximately 396,016 m², this study focused specifically on the 79,941 m² core campus area, which serves as the primary center of academic activities and exhibits the highest development intensity. The core campus area was selected because it is predominantly occupied by buildings, asphalt roads, and paved surfaces and is therefore more susceptible to land cover changes associated with future development. Accordingly, this area was considered representative for evaluating the relationship between land cover change, infiltration capacity, and surface runoff generation using the Horton Model.

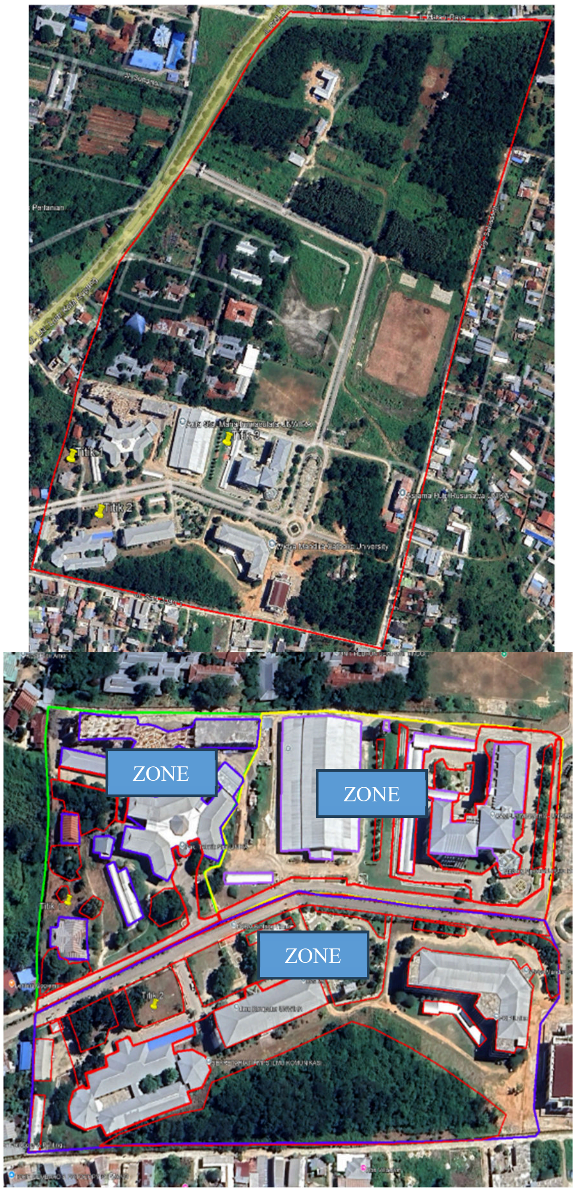

Figure 1. Study area

The data collected in this study consisted of both primary and secondary data. Primary data were obtained through field measurements of infiltration rates using a double-ring infiltrometer at three observation points representing vegetated land, semi-permeable land, and built-up land. Secondary data included: Daily maximum rainfall records obtained from the Lasiana Climatological Station (BMKG); Campus land-use data provided by the University's Planning Division; Measurements of built-up and open-space areas within the campus (in hectares); and topographic maps and land-use maps.

Analysis procedures

Measurement of infiltration rate

The field infiltration rate was calculated based on the decline in the water level over time using the following equation (ASTM International 2018):

$$f_{obs} = \frac{\Delta h}{\Delta t} \quad (1)$$

Where: $fobs$ = observed infiltration rate (cm/hour); Δh = observed infiltration rate (cm/hour); and Δt = observation time interval (hour).

Application of the Horton Model

The Horton infiltration equation is expressed as follows (Horton R.E, 1941):

$$f(t) = f_c + (f_0 - f_c)e^{-kt} \quad (2)$$

where: ft = infiltration rate at time t (cm/hour); $f0$ = initial infiltration rate (cm/hour); fc = constant infiltration rate (cm/hour); k = decay constant; and t = time (hour).

To calculate cumulative infiltration over the rainfall duration, the following equation was used:

$$F(t) = f_c t + \frac{(f_0 - f_c)}{k}(1 - e^{-kt}) \quad (3)$$

Where: Ft = cumulative infiltration (cm or mm). The parameters $f0$, fc, and k were calibrated using a model optimization approach that minimized the error between the observed data and the model predictions.

Calculation of Infiltration Volume and Surface Runoff

The infiltration volume was calculated from the cumulative infiltration obtained using the Horton Model (Horton 1941), and subsequently compared with the design rainfall corresponding to the 2-year (R_2), 5-year (R_5), and 10-year (R_{10}) return periods.

The rainfall volume for each land-cover type was determined using the following equations:

$$V_h = \frac{P}{1000} \times A \quad (4)$$

$$V_{inf} = \frac{F_t}{1000} \times A_p \quad (5)$$

$$V_{limp} = \max(0, V_{masuk} - V_{inf}) \quad (6)$$

$$Q = \frac{V_{limp}}{t} \quad (7)$$

Where: $Vinf$ = infiltration volume (m³); Ft = cumulative Horton infiltration (mm); Ap = permeable area (m²); P = design rainfall (mm); Q = average runoff discharge (m³/s); and t = rainfall duration (seconds).

Model evaluation and validation

The model performance was evaluated using absolute error, percentage error, and the Root Mean Square Error (RMSE) (Moriasi et al. 1983).

The absolute error was calculated as:

$$E_i = f_{model,i} - f_{obs,i} \quad (8)$$

The percentage error was calculated as:

$$\%E_i = \frac{f_{model,i} - f_{obs,i}}{f_{obs,i}} \times 100\% \quad (9)$$

The RMSE was calculated using the following equation:

$$RMSE = \sqrt{\frac{1}{n}\sum_{i=1}^{n}(f_{model,i} - f_{obs,i})^2} \quad (10)$$

Where: Ei = error associated with the i–th observation; $fmodel$, i = infiltration value predicted by the model for the i-th observation; $fobs$, i = observed infiltration value for the i-th observation; and n = number of observations.

In addition, the model performance was evaluated through residual plots and by comparing the observed infiltration rates with those predicted by the Horton Model.

Sensitivity analysis of land cover change

The sensitivity analysis was performed by simulating the gradual conversion of permeable land into built-up areas by 1%, 2%, 3%, 4%, and 5% relative to the existing land-cover condition.

The permeable area after land-cover change was calculated using the following equation (Mejía and Moglen 2010):

$$A_{p,s} = A_{p,0}(1 - r) \quad (11)$$

Where: Ap, s = permeable area under the simulated scenario (m²); Ap,0 = existing permeable area (m²); and r = percentage of land-cover change.

The infiltration capacity under each scenario was calculated as:

$$V_{inf,s} = \frac{F_t}{1000} \times A_{p,s} \quad (12)$$

The runoff volume for each scenario was calculated as:

$$V_{limp,s} = V_{masuk} - V_{inf,s} \quad (13)$$

or alternatively,

$$V_{limp,s} = \max(0, V_{masuk} - V_{inf,s}) \quad (14)$$

The percentage increase in runoff resulting from land-cover change was determined using:

$$\Delta V_{limp} = \frac{V_{limp,s} - V_{limp,0}}{V_{limp,0}} \times 100\% \quad (15)$$

Where: $Vlimp$, s = runoff volume under the simulated land-cover scenario (m³); and $Vlimp$,0 = runoff volume under the existing condition (m³).

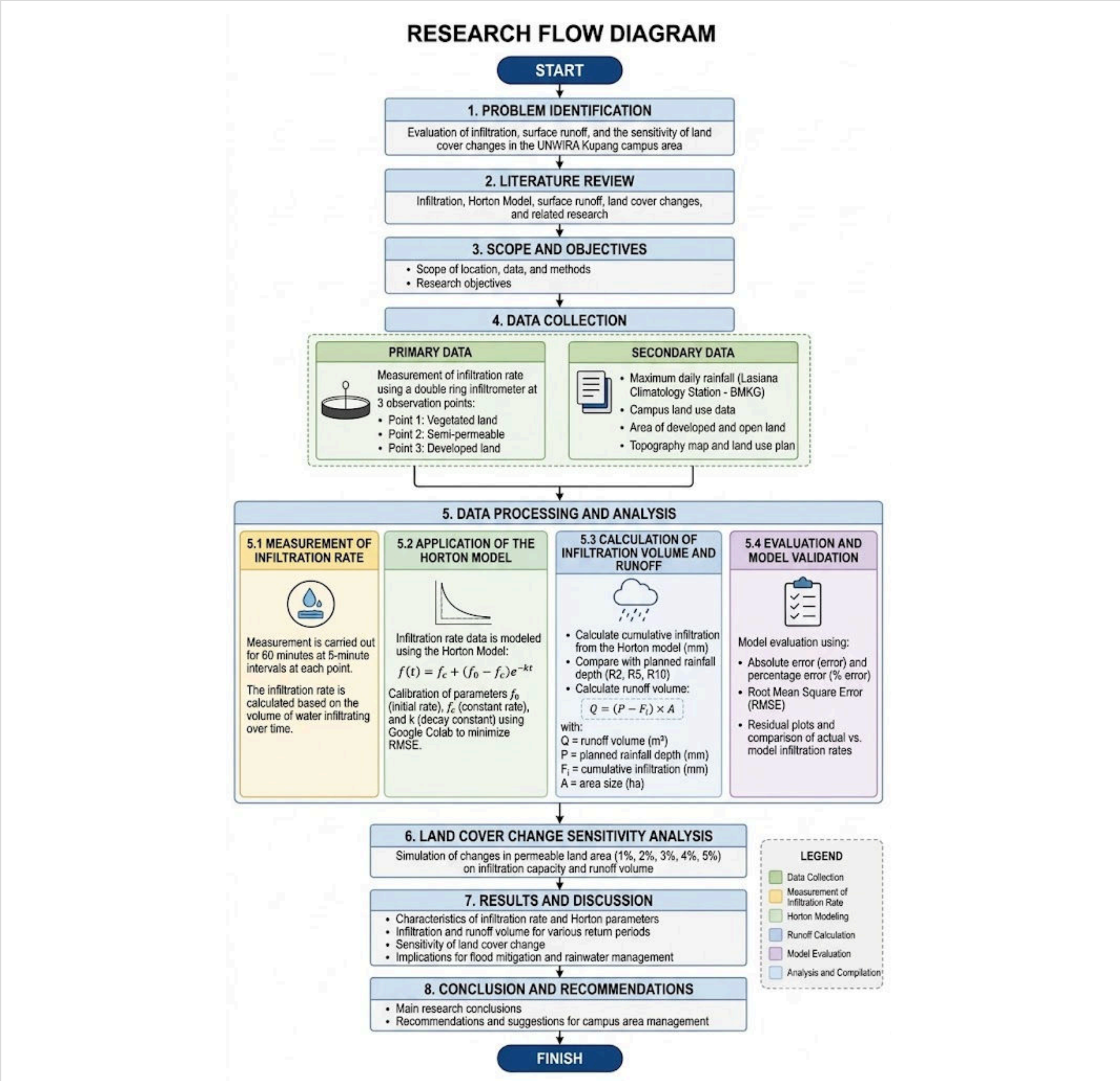

Figure 2. Research flowchart

RESULTS AND DISCUSSIONN

Field infiltration measurement results

The field measurements revealed a progressive decline in infiltration rate over time that consistently followed an exponential pattern, thereby supporting the applicability of the Horton Model.

Table 1. Field infiltration rate measurement results

Time (minutes)	Time (hours)	Water Level Decline at Point 1 (cm)	Water Level Decline at Point 2 (cm)	Water Level Decline at Point 3 (cm)
0	0.00	—	—	—
5	0.08	15.0	13.0	14.0
10	0.17	14.5	12.5	12.5
15	0.25	12.5	10.0	10.0
20	0.33	10.0	8.0	9.0
25	0.42	8.5	6.0	7.0
30	0.50	4.0	4.0	6.0
35	0.58	2.5	3.5	4.5
40	0.67	2.5	3.5	4.5
45	0.75	2.5	3.5	4.5

https://doi.org/10.59810/lejlace.v4i2.276

For a 5-minute observation interval, the infiltration rate is calculated as:

$$f_i = \frac{\Delta h_i}{\Delta t}$$

where:

$$\Delta t = \frac{5}{60} = 0{,}08333 \text{ hour}$$

If the field measurements are recorded in millimeters, then:

$$f_i = \frac{\Delta h_i/10}{5/60} = 1{,}2\Delta h_i$$

For Point 1:

$$f_1 = 1{,}2(15) = 18 \text{ cm/hour}$$

Accordingly, the corrected infiltration rates are presented below.

Table 2. Infiltration rate at each observation point

Time	Point 1	Point 2	Point 3
5 minutes	18.00	15.60	16.80
10 minutes	17.40	15.00	15.00
15 minutes	15.00	12.00	12.00
20 minutes	12.00	9.60	10.80
25 minutes	10.20	7.20	8.40
30 minutes	7.20	4.80	7.20
35 minutes	3.00	4.20	5.40
40 minutes	3.00	4.20	5.40
45 minutes	3.00	4.20	5.40

After the observed infiltration rates had been determined, the data for each observation interval were represented at the midpoint of the corresponding time interval (i.e., 2.5–42.5 minutes) and subsequently modeled using the Horton equation:

$$f(t) = f_c + (f_0 - f_c)e^{-kt}$$

The value of fc was determined from the average of the final three measurements after the infiltration rate had stabilized, whereas $f0$ and k were obtained through nonlinear optimization by minimizing the RMSE between the model predictions and the observed infiltration data. The calibration results demonstrated that the Horton Model effectively represented the decline in infiltration rate at all three observation points. The highest level of agreement was achieved at Point 3, with an RMSE of 0.894 cm/hour, followed by Point 2 with 1.289 cm/hour, and Point 1 with 2.001 cm/hour. The comparison between the observed infiltration rates and the Horton Model predictions is presented in figure 3.

Table 3. Summary of Horton Model parameters

Observation Point	f_0 (cm/hour)	f_c (cm/hour)	k (hour^{-1})	RMSE (cm/hour)
Point 1	22.90	3.00	3.371	2.001
Point 2	19.72	4.20	4.267	1.289
Point 3	20.11	5.40	4.231	0.894

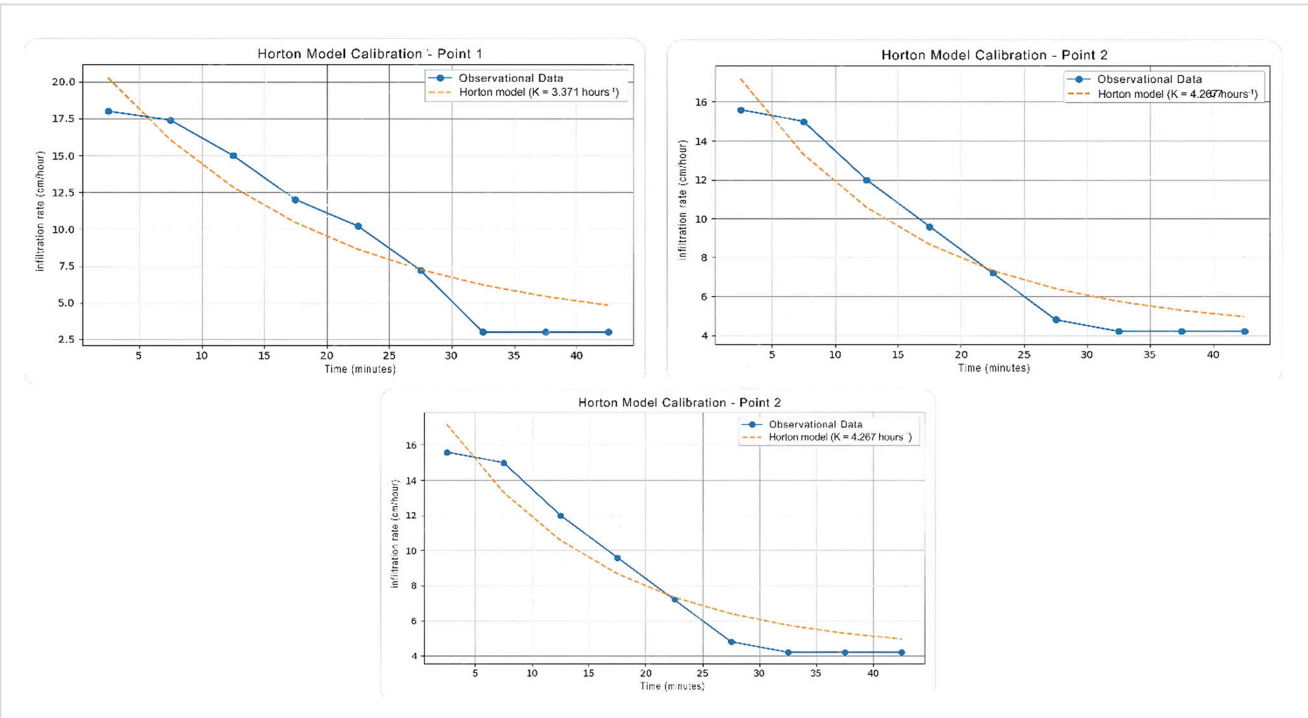

Figure 3. Horton Model Calibration Curves for Observation Points 1, 2, and 3

Figure 3 illustrates that the Horton Model successfully captures the declining trend in infiltration rates at all three observation points. The best agreement between the model and the observed data was obtained at Point 3, with an RMSE of 0.894 cm/hour, followed by Point 2 (1.289 cm/hour) and Point 1 (2.001 cm/hour). Differences between the model predictions and field observations are primarily evident during the transition phase toward the steady-state infiltration condition. Nevertheless, the modeled curves generally reproduce the observed infiltration behavior satisfactorily. Based on the calibrated parameters, the cumulative infiltration over a 60-minute period was 8.70 cm, 7.79 cm, and 8.83 cm for Point 1, Point 2, and Point 3, respectively. These values served as the basis for calculating the infiltration capacity of each zone and estimating the corresponding surface runoff.

Design rainfall analysis

The analysis of maximum daily rainfall data collected over a ten-year period from the El Tari and Lasiana Meteorological Stations yielded average annual maximum rainfall values of 172 mm and 138 mm, respectively, resulting in a combined average of 155.0 mm, which served as the basis for the design rainfall analysis. Four probability distributions, Normal, Log Normal, Gumbel, and Log Pearson Type III, were evaluated using the Chi-Square and Smirnov–Kolmogorov goodness-of-fit tests.

Based on the statistical parameters C_s, C_k, and C_v, the Log Pearson Type III distribution best satisfied the selection criteria and was therefore adopted for the estimation of design rainfall.

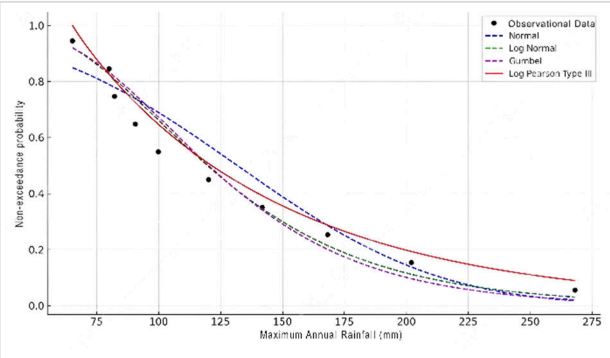

Figure 4. Comparison of rainfall probability distributions

Figure 4 demonstrates that the Log Pearson Type III distribution most closely matches the observed rainfall data compared with the Normal, Log Normal, and Gumbel distributions. The Chi-Square test yielded a value of $\chi_{\text{"calculated"}}^2=2,000$, which is lower than $\chi_{\text{"critical"}}^2=5,991$, while the Smirnov–Kolmogorov test produced $D_{max}=0,020202$, which is smaller than the critical value $D_0=0,410$. Figure 4 demonstrates that the Log Pearson Type III distribution most closely matches the observed rainfall data compared with the Normal, Log Normal, and Gumbel distributions. The Chi-Square test yielded a value of.

Table 4. Rainfall intensity analysis using the Mononobe method

Duration (minutes)	R_2 (mm/hour)	R_5 (mm/hour)	R_{10} (mm/hour)
60	39.945	59.834	75.576
120	25.163	37.693	47.610
180	19.203	28.765	36.333
240	15.852	23.745	29.993
300	13.661	20.463	25.847

Figure 5 illustrates the relationship between rainfall duration and rainfall intensity for the 2-year, 5-year, and 10-year return periods based on the Mononobe Method. The figure clearly indicates that rainfall intensity decreases as rainfall duration increases for all return periods. At a rainfall duration of 60 minutes, rainfall intensity reaches its maximum values of 39.95 mm/hour, 59.83 mm/hour, and 75.58 mm/hour for the 2-year, 5-year, and 10-year return periods, respectively. As rainfall duration increases to 300 minutes, the corresponding rainfall intensities gradually decrease to 13.66 mm/hour, 20.46 mm/hour, and 25.85 mm/hour for the respective return periods. This trend indicates that shorter-duration rainfall events tend to exhibit considerably higher rainfall intensities, whereas longer-duration storms generally produce lower rainfall intensities.

Surface Runoff analysis

The study area was divided into three zones according to land-use characteristics, surface drainage patterns, and the locations of the infiltration test points representing each zone. An inventory was subsequently conducted to determine the areas occupied by building roofs, asphalt pavements, paved roads, open land, and vegetated areas, providing the basis for calculating rainfall volume associated with each land-cover type. The summary of land-cover areas for each zone is presented in table 5.

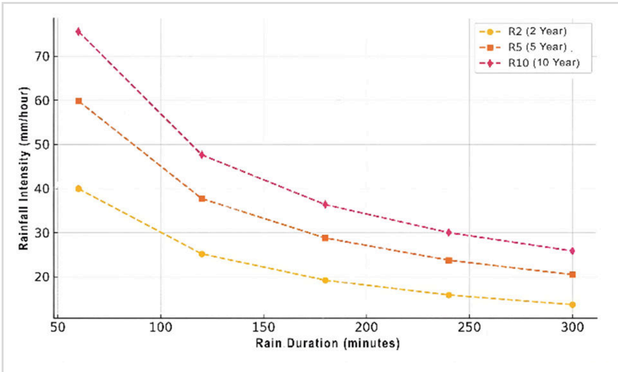

Figure 5. Rainfall intensity for each return period

Table 5. Land cover area of each zone

Parameter	Zone 1	Zone 2	Zone 3
Total area (m²)	17,076	40,260	22,605
Roof area (m²)	6,216.0	8,381.2	7,700.2
Asphalt road area (m²)	1,158	2,751	2,158
Paved area (m²)	453	1,871	4,805
Open land (m²)	7,152.0	15,836.8	7,126.8
Vegetated area (m²)	2,097	11,420	815

As shown in table 5, Zone 2 encompasses the largest area, totaling 40,260 m², equivalent to approximately 50.37% of the entire study area. This zone also contains the largest roof area and the greatest extent of vegetated land compared with the other two zones. In contrast, Zone 1 is dominated by existing buildings and relatively limited open space, whereas Zone 3 contains the highest proportion of paved surfaces. These differences in land-cover composition indicate that each zone contributes differently to surface runoff generation. Consequently, runoff analyses were conducted separately for each zone according to its specific land-use characteristics.

Surface runoff was estimated for a 60-minute rainfall duration using the most recently calibrated Horton Model parameters.

https://doi.org/10.59810/lejlace.v4i2.276

Zone 1 was represented by Point 1, Zone 2 by Point 3, and Zone 3 by Point 2. The calibrated parameters and cumulative infiltration values used in the analysis were as follows:

- Point 1: $f_0 = 22{,}90$cm/hour, $f_c = 3{,}00$cm/hour, $k = 3{,}371$hour $^{-1}$, and $F_{60} = 8{,}70$cm;
- Point 2: $f_0 = 19{,}72$cm/hour, $f_c = 4{,}20$cm/hour, $k = 4{,}267$hour $^{-1}$, and $F_{60} = 7{,}79$cm;
- Point 3: $f_0 = 20{,}11$cm/hour, $f_c = 5{,}40$cm/hour, $k = 4{,}231$hour $^{-1}$, and $F_{60} = 8{,}83$cm.

The infiltration capacity was calculated based on cumulative infiltration and the corresponding permeable area, whereas runoff volume was determined from the difference between the incoming rainfall volume and the infiltration capacity. The calculation results are summarized in table 6.

Table 6. Summary of estimated surface runoff for each zone

Zone	Representative Point	Infiltration Capacity (m³)	Runoff R_2 (m³)	Runoff R_5 (m³)	Runoff R_{10} (m³)	Discharge R_2 (m³/s)	Discharge R_5 (m³/s)	Discharge R_{10} (m³/s)
Zone 1	Point 1	804.58	0.00	217.15	485.96	0.0000	0.0603	0.1350
Zone 2	Point 3	2,405.42	0.00	3.50	637.27	0.0000	0.0010	0.1770
Zone 3	Point 2	618.33	284.63	734.22	1,090.07	0.0791	0.2040	0.3028

The runoff estimation indicates that Zone 3 generated the greatest runoff volumes for all return periods because it possesses the lowest infiltration capacity. Zone 1 produced no runoff under the R_2 rainfall event; however, runoff increased substantially under the R_5 and R_{10} scenarios. Zone 2 exhibited the highest infiltration capacity, although runoff began to occur under the R_5 rainfall event and increased to 637.27 m³ under the R_{10} scenario.

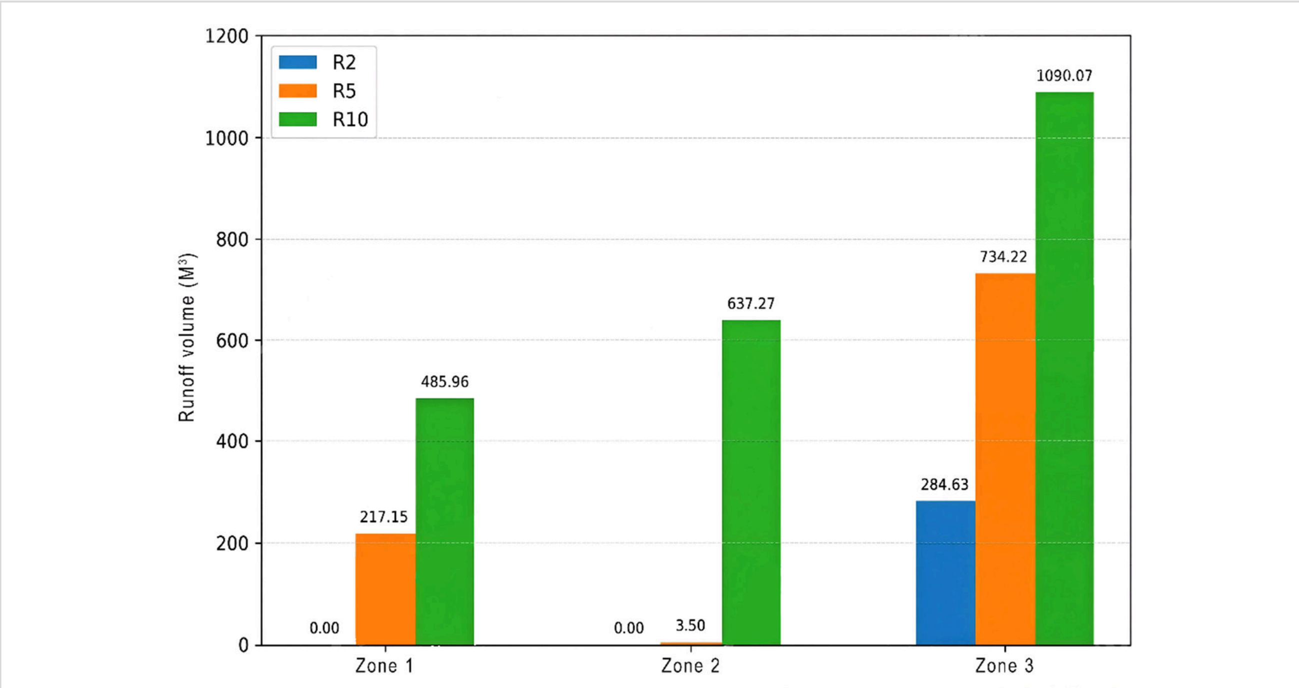

Figure 6. Comparison of surface runoff among the three zones

Figure 6 demonstrates that runoff volume increases progressively with increasing rainfall return period. Zone 1 generated no runoff under the R_2 event, but runoff reached 217.15 m³ under R_5 and increased to 485.96 m³ under R_{10}. Zone 2, which exhibited the highest infiltration capacity (2,405.42 m³), produced no runoff under R_2, only 3.50 m³ under R_5, and 637.27 m³ under R_{10}. In contrast, Zone 3 proved to be the most vulnerable area because it possessed the lowest infiltration capacity (618.33 m³), resulting in runoff volumes of 284.63 m³, 734.22 m³, and 1,090.07 m³ under the R_2, R_5, and R_{10} rainfall events, respectively. These findings demonstrate that the extent of permeable land and infiltration capacity plays a decisive role in determining runoff volume. Consequently, zones with limited infiltration capacity experience more rapid increases in surface runoff and are therefore more susceptible to localized flooding.

Sensitivity analysis of land cover change on surface runoff

To evaluate the hydrological response of the study area to land cover change, a sensitivity analysis was conducted by simulating the gradual conversion of permeable land into built-up areas at increments of 1%, 2%, 3%, 4%, and 5% of the existing permeable area in each study zone. For every simulation scenario, the Horton Model infiltration parameters (f_0, f_c, and k) were assumed to remain constant, while only the extent of the permeable area was modified. The results of each simulation scenario were then used to evaluate the increase in surface runoff resulting from the reduction in permeable land and to identify the relative vulnerability of each zone to future built-up development.

Table 7. Land cover change scenarios

Scenario	Change in Permeable Area	Built-up Area
Existing	0%	100% existing condition
S1	1%	1%
S2	2%	2%
S3	3%	3%
S4	4%	4%
S5	5%	5%

The 1–5% range of land-cover change was selected to represent realistic incremental changes resulting from the construction of new buildings, expansion of parking areas, and the development of supporting campus facilities. This range was adopted to evaluate the sensitivity of the Horton Model to relatively small-scale land-cover modifications and to determine how rapidly the campus infiltration capacity decreases and runoff volume increases as permeable land is progressively converted into impervious built-up areas. Sensitivity and Vulnerability.

Analysis Across the Three Zones

- Zone 2 exhibited the highest relative sensitivity, with runoff increasing by 18.87% under the scenario involving a 5% reduction in permeable area.
- Zone 3 proved to be the most hydrologically vulnerable, as it already generated the largest existing runoff volume under the R_{10} rainfall event, reaching 1,090.07 m³.
- Zone 1 exhibited an intermediate level of sensitivity, with runoff increasing by 8.28% under the 5% land-cover change scenario.

Table 8. Comparison of land cover change sensitivity among the three zones

Parameter	Zone 1	Zone 2	Zone 3
Existing permeable area (m²)	9,249.00	27,256.80	7,941.80
Existing infiltration capacity (m³)	804.58	2,405.42	618.33
Existing runoff under R_{10} (m³)	485.96	637.27	1,090.07
Runoff under the 5% scenario (m³)	526.19	757.54	1,120.99
Additional runoff (m³)	40.23	120.27	30.92
Increase in runoff (%)	8.28	18.87	2.84
Principal characteristic	Moderate sensitivity	Highest relative sensitivity	Highest actual vulnerability

The comparative analysis demonstrates that Zone 2 is the most sensitive in relative terms, exhibiting an 18.87% increase in runoff, from 637.27 m³ to 757.54 m³, under the scenario involving a 5% reduction in permeable area. Although Zone 3 experienced the smallest relative increase (2.84%), it remained the most hydrologically vulnerable zone because its runoff volume increased from 1,090.07 m³ to 1,120.99 m³, representing the largest absolute runoff volume among all study zones. Meanwhile, Zone 1 displayed an intermediate response, with runoff increasing by 8.28%, from 485.96 m³ to 526.19 m³.

These findings demonstrate that relative sensitivity and hydrological vulnerability are not necessarily equivalent. While Zone 2 responds most strongly to incremental land-cover change on a percentage basis, Zone 3 remains the most critical area from a stormwater management perspective because of its substantially larger runoff volume. Consequently, planning decisions should consider both relative sensitivity and actual runoff magnitude when establishing priorities for sustainable campus development and stormwater mitigation.

CONCLUSION

Conclusions

Based on the field measurements, Horton Model calibration, design rainfall analysis, runoff estimation, and land-cover change simulations, the following conclusions can be drawn: (1) The Horton Model successfully represented the declining trend of infiltration rates at all three observation points, yielding RMSE values ranging from 0.894 to 2.001 cm/hour, thereby demonstrating satisfactory agreement between the model predictions and the field observations. (2) Zone 2 exhibited the greatest infiltration capacity, amounting to 2,405.42 m³, whereas Zone 3 generated the highest runoff volume under the R_{10} rainfall event, reaching 1,090.07 m³, making it the most vulnerable zone to surface ponding and localized flooding; (3) Under the scenario involving a 5% reduction in permeable area, Zone 2 exhibited the highest relative sensitivity, with runoff increasing by 18.87%, whereas Zone 3 remained the most critical zone based on the magnitude of its actual runoff volume.

Recommendations

Based on the findings of this study, the following recommendations are proposed: (1) The permeable area within Zone 2 should be preserved, as it functions as the principal infiltration zone within the campus and plays a crucial role in reducing surface runoff; (2) Zone 3 should receive the highest priority for stormwater management interventions, including the installation of infiltration wells, biopore infiltration systems, permeable pavements, temporary detention facilities, and improvements to the existing drainage network; (3) Future building development in all campus zones should be accompanied by adequate infiltration facilities to compensate for the reduction in permeable land resulting from ongoing urban development; (4) Future studies should increase the number of infiltration testing locations and integrate runoff estimation with the hydraulic capacity of the existing campus drainage network, thereby enabling a more comprehensive evaluation of stormwater management performance under future land-use scenarios.

https://doi.org/10.59810/lejlace.v4i2.276

REFERENSI

Annisa, Bismi. 2018. "Penerapan Model Horton Untuk Kuantifikasi Laju Infiltrasi." *JURNAL SAINTIS* 18 (1): 95–102. https://doi.org/10.25299/saintis.2018.vol18(1).3198.

ASTM International. 2018. "Test Method for Infiltration Rate of Soils in Field Using Double-Ring Infiltrometer." West Conshohocken, PA: ASTM International. https://doi.org/10.1520/D3385-18.

Bagus, M., S. Putra, M. N. Trilita, and Wahjudijanto. 2022. "Analisa Debit Banjir Rencana Pada Daerah Aliran Sungai Banyumileng."

Christian, Christian, and Wati Asriningsih Pranoto. 2021. "ANALISIS PENYEBAB BANJIR DAN SOULSINYA PADA PERUMAHAN KFT- CENGKARENG BARAT." *JMTS: Jurnal Mitra Teknik Sipil* 4 (2): 455. https://doi.org/10.24912/jmts.v0i0.10544.

Felix, Lionel, and Gregorius Sandjaja Sentosa. 2020. "SIMULASI SUMUR RESAPAN BERDASARKAN ANALISIS PERBANDINGAN KETINGGIAN AIR BANJIR DI KELAPA GADING JAKARTA." *JMTS: Jurnal Mitra Teknik Sipil* 3 (3): 797. https://doi.org/10.24912/jmts.v3i3.8289.

Horton, Robert E. 1941. "An Approach Toward a Physical Interpretation of Infiltration-Capacity." *Soil Science Society of America Journal* 5 (C): 399–417. https://doi.org/10.2136/sssaj1941.036159950005000C0075x.

Mejía, Alfonso I., and Glenn E. Moglen. 2010. "Impact of the Spatial Distribution of Imperviousness on the Hydrologic Response of an Urbanizing Basin." *Hydrological Processes* 24 (23): 3359–73. https://doi.org/10.1002/hyp.7755.

Moriasi, D. N., J. G. Arnold, M. W. Van Liew, R. L. Bingner, R. D. Harmel, and T. L. Veith. 1983. "Model Evaluation Guidelines for Systematic Quantification of Accuracy in Watershed Simulations." *Transactions of the ASABE* 50 (3): 885–900. https://doi.org/10.13031/2013.23153.

Suryanto, Joko. 2017. "Penentuan Laju Irigasi Di Lahan Pertanian Kecamatan Sangatta Selatan Menggunakan Model Infiltrasi Terpilih." *Jurnal Pertanian Terpadu* 5 (1): 56–67.

Yang, Moyuan, Yongyong Zhang, and Xingyao Pan. 2020. "Improving the Horton Infiltration Equation by Considering Soil Moisture Variation." *Journal of Hydrology* 586 (July):124864. https://doi.org/10.1016/j.jhydrol.2020.124864.

This page is intentionally left blank

https://doi.org/10.59810/lejlace.v4i2.276